Article

Chinese Science Bulletin

Theoretical Chemistry

February 2012 Vol.57 No.4: 328–335
doi: 10.1007/s11434-011-4797-0

Theoretical characterization of single-electron iodine-bond weak interactions in $CH_3\cdots I—Y$(Y = BH_2, H, CH_3, C_2H_3, C_2H, CN, NC) systems

YUAN Kun[1,2*], LIU YanZhi[1,2], ZHU YuanCheng[1,2], ZUO GuoFang[1,2], LÜ LingLing[1,2] & LI ZhiFeng[1]

[1] *College of Life-science and Chemistry, Tianshui Normal University, Tianshui 741001, China;*
[2] *Key Laboratory for New Molecular Materials Design and Function of Gansu Education Department, Tianshui 741001, China*

Received January 12, 2011; accepted June 22, 2011

Iodine-involved single-electron halogen bonds (SEXBs) weak interactions in the systems of $CH_3\cdots I—Y$(Y = BH_2, H, CH_3, $CH{=}CH_2$, $C{\equiv}CH$, CN, NC) were investigated for the first time using B3LYP/6-311++G(d,p) and MP2/aug-*cc*-pVTZ computational levels (the relativistic effective core potential basis set of Lanl2dz was used on iodine atom). The interaction energies between two moieties with basis set super-position error corrections for the seven complexes are −0.57, −1.36, −3.80, −2.17, −4.49, −6.33 and −8.64 kJ mol^{-1} (MP2/aug-*cc*-pVTZ), respectively, which shows that SEXBs interactions are all weak. Natural bond orbital theory analysis revealed that charges flow from CH_3 to the I—Y moiety. The total amount of natural bond orbital charge transfer (Δ_{NC}) from the CH_3 radical to I—Y increases in the order $CH_3\cdots IBH_2 < CH_3\cdots IH \approx CH_3\cdots ICH_3 \approx CH_3\cdots IC_2H_3 < CH_3\cdots ICCH < CH_3\cdots ICN < CH_3\cdots INC$. Atoms-in-molecules theory was used to investigate the topological properties of the bond critical points in the seven SEXB structures.

CH_3 radical, single-electron iodine-bond, natural bond orbital analysis, electron density topological property

Citation: Yuan K, Liu Y Z, Zhu Y C, et al. Theoretical characterization of single-electron iodine-bond weak interactions in $CH_3\cdots I—Y$(Y= BH_2, H, CH_3, C_2H_3, C_2H, CN, NC) systems. Chin Sci Bull, 2012, 57: 328–335, doi: 10.1007/s11434-011-4797-0

Noncovalent weak interactions have important roles in the field of molecule recognition, in biological systems, and in materials science. These interactions have captured the interest of chemists for a long time, and studies of their theories and experiments have been well reported [1]. It has been found that many physical and chemical phenomena are closely related to intermolecular noncovalent weak interactions including dihydrogen bonds [2], π-cation interactions [3], halogen bonds (XB) [4], lithium bonds [5]. Recently, single-electron noncovalent bonds have been the most extensively studied noncovalent interaction [6–9]. Most published work is on single-electron noncovalent bonds of the type $CH_3\cdots M—Y$ (M = H, Li, F, Cl or Br), in which the single electron of the CH_3 radical, acting as the electron donor (but the halogen bond acceptor), interacts with the M—Y moiety, acting as the electron acceptor (but the halogen bond donor), as shown in Figure 1. The single-electron halogen-bond (SEXB) interaction is one of these single-electron noncovalent interactions. However, only the single-electron bromine-bond has been studied [10–12], and neither experimental nor theoretical studies of the other SEXBs involving iodine have been reported. It is known that the iodine atom has more polarity and distortion than bromine atom. Thus iodine would be more suitable than bromine atom as an electron acceptor in SEXB systems. Based on these ideas, we are interested in whether there are any iodine-involved SEXB interactions, and how the interactions take place. We consider a particular set of molecules

*Corresponding author (email: yuankun@tscn.edu.cn)

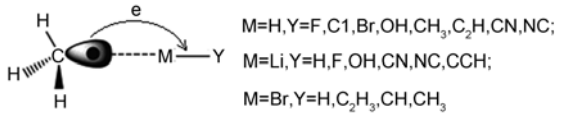

Figure 1 The representation of single-electron noncovalent bond between CH_3 radical and M—Y.

formed by a "donor" (CH_3 radical) and "acceptors" of electrons, as shown in Figure 2, where the iodine atoms in I—Y (Y = BH_2, H, CH_3, CH═CH_2, C≡CH, CN, and NC) are electronically poor enough to accept the single electron of the CH_3 radical to form an SEXB. Thus, given the absence of both experimental and theoretical studies on iodine-involved SEXB interactions of CH_3 with I—Y (Y = BH_2, H, CH_3, CH═CH_2, C≡CH, CN, and NC), the present study reports the nature of these interactions, characterized using the density functional Becke, three-parameter, Lee-Yang-Parr (B3LYP) and second-order Møller-Plesset (MP2) theoretical methods.

1 Computational details

All the monomers and complexes were optimized using the density functional B3LYP and the MP2 methods. The relativistic effective core potential (ECP) basis set of Lanl2dz was used on the iodine atoms, and the 6-311++G(d,p) and aug-*cc*-pVTZ were used on the other atoms. These methods and basis sets have recently been shown to adequately describe noncovalent interaction systems [13–15]. Thus they are reliable for the purpose of our study. Harmonic frequency analyses were performed at the same levels to confirm that these structures were local minima on the energy surfaces. The interaction energies were corrected with the basis set superposition error (BSSE). The BSSE was evaluated using the counterpoise method of Boys and Bernardi [16]. The atoms-in-molecules (AIM) theory of Bader [17] was used to find the bond critical points (BCP) and to analyze them in terms of electron densities and their Laplacians. The AIM calculations were carried out with the AIM 2000 program [18]. Natural bond orbital (NBO) analyses were carried out with the NBO 5.0 package [19]. All other calculations were performed with the Gaussian 03 program [20].

2 Results and discussion

2.1 Geometric configuration and frequency analysis

The B3LYP method has proved to be reliable during geometric

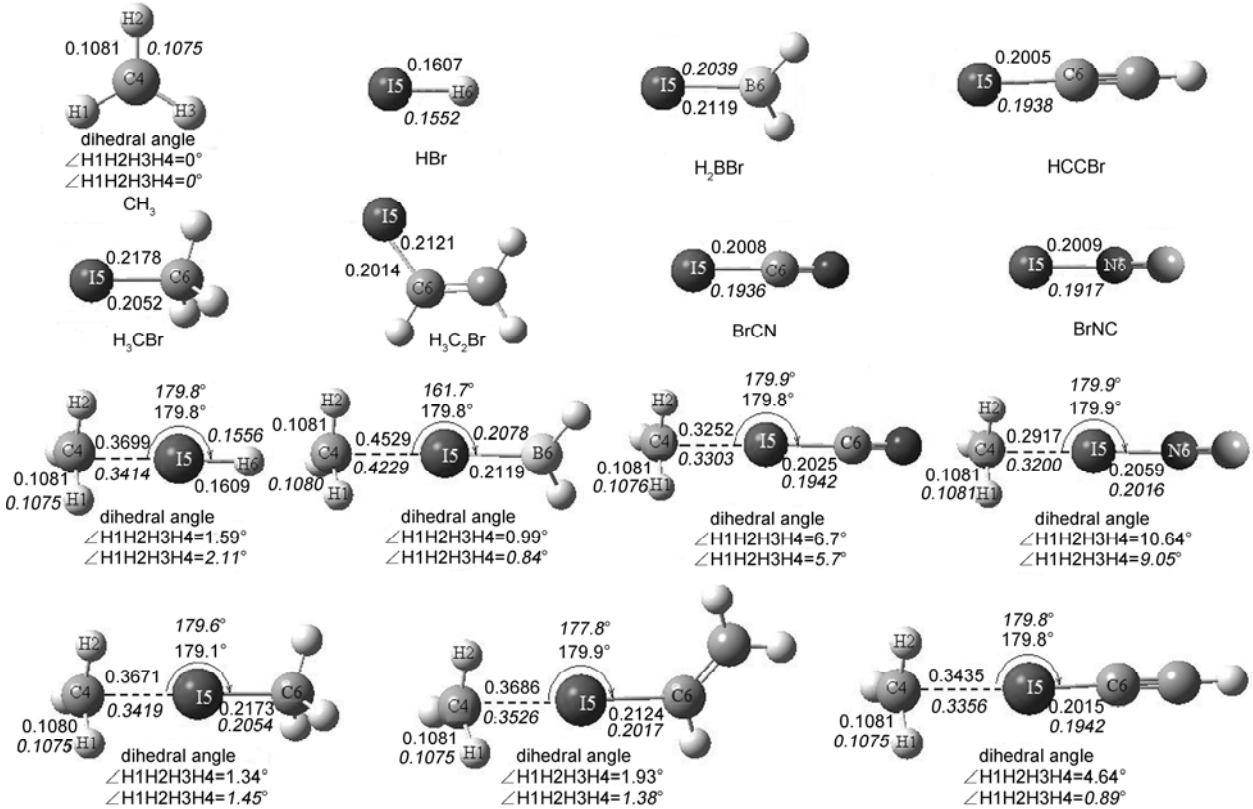

Figure 2 Geometries (bond length in nm, bond angle and dihedral angle in (°)) of the CH_3···I—Y(Y = BH_2, H, CH_3, C_2H_3, CCH, CN, and NC) complexes calculated at B3LYP/6-311++G**(in regular type) and MP2/aug-*cc*-pVTZ (in italics) levels.

optimization and transition state calculations [13], and the MP2 method has been used successfully to study weak interactions [15]. The optimized geometric configurations on the potential surfaces of the monomers and $CH_3\cdots I—Y$(Y = BH_2, H, CH_3, C_2H_3, CCH, CN and NC) complexes are shown in Figure 2, and some important structural parameters obtained at the B3LYP/6-311++G** (in regular type) and MP2/aug-*cc*-pVTZ (in italics) computational levels are also shown. As shown in Figure 2, the seven complexes all have C_1 symmetry, and the parameters obtained at the B3LYP/6-311++G** level agree with those calculated by MP2/aug-*cc*-pVTZ. In the 7 complexes, SEXBs were formed via the IY(Y = BH_2, H, CH_3, C_2H_3, CCH, CN, and NC) as the electron acceptor (SEXB donor) and the C atom of CH_3 as electron donor. The van der Waals radius is an important factor in investigating the geometric structure. If the distance between two atoms is obviously less than the sum of their van der Waals radius, a certain degree of weak interaction from hydrogen bonding or halogen bonding, which is stronger than van der Waals forces, exists between the two atoms. Here, the C···I distances in the complexes of $CH_3\cdots I—H$, $CH_3\cdots I—CH_3$, $CH_3\cdots I—CHCH_2$, $CH_3\cdots I—CCH$, $CH_3\cdots I—CN$ and $CH_3\cdots I—NC$ obtained at the B3LYP/6-311++G** level are 0.3699, 0.3671, 0.3686, 0.3435, 0.3252 and 0.2917 nm, respectively, which are all less than the sum of the van der Waals radii of the carbon atom (0.170 nm) and the iodine atom (0.198 nm) [21]; this is part of the evidence for the existence of single-electron iodine-bond interactions. The C···I bond distances in the present study are shorter than the C···Br bond lengths reported for single-electron Br-bond systems in our previous study [11]. Furthermore, the bond angles among the three atoms involved in SEXBs are all close to 180°, and the two moieties exhibit "T" shapes in space.

In addition, the CH_3 moiety has a planar configuration, and the dihedral angle among its four atoms is 0°, but the structural parameters of the seven $CH_3\cdots I—Y$ complexes show that the C atoms of the CH_3 fragment should have hybridization between sp^2 and sp^3. In fact, the calculation results support this. For example, the hybridization of the C atom in the $CH_3\cdots INC$ complex is $sp^{2.1}$, and the dihedral angle among the four atoms of the CH_3 fragment is about 10°, which is obviously larger than that of the CH_3 moiety. This suggests the existence of a C···I SEXB between the two moieties. The relationship between the dihedral ∠H1H2H3C4 and $d_{C\cdots I}$ is given in Figure 3; it can be seen that the larger the dihedral ∠H1H2H3C4 is, the larger the $d_{C\cdots I}$ is. Comparing parameters of the moieties with those of the complexes given in Figure 2, it can be easily found that the I—Y bond lengths all increased to some degree after complex formation at the two theoretical computation levels. For example, the I—C bond lengths increased by 0.0003, 0.001, and 0.0017 nm at the B3LYP/6-311++G** level in the complexes $CH_3\cdots IC_2H_3$, $CH_3\cdots ICCH$, and $CH_3\cdots ICN$, respectively. In particular, the I—N bond length increased

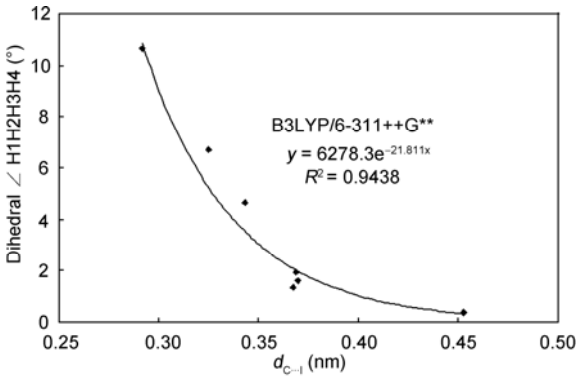

Figure 3 Relationship between dihedral ∠H1H2H3C4 and $d_{C\cdots I}$.

by as much as 0.005 nm at the B3LYP/6-311++G** level in the complex $CH_3\cdots INC$. This predicts an obvious red-shift of its stretching vibrational frequency after the SEXB complex is formed.

To help with possible experimental identification of the SEXB structures described in this work, Table 1 shows the corresponding bond stretching vibrational intensities and frequencies of the monomers and SEXB complexes calculated at the B3LYP/6-311++G** and MP2/aug-*cc*-pVTZ levels. The frequency analysis shows that the SEXB configurations are all stable points on the potential surfaces of the complexes, except for $CH_3\cdots ICH_3$, which is a transition point. Although the data obtained using B3LYP and MP2 are not always in agreement, it is found that the stretching vibrational frequency of the I—Y bond in the $CH_3\cdots INC$ complex presents an obvious red-shift. As shown in Figure 4, we also noted that the C···I stretching vibrational frequencies ($\upsilon_{C\cdots I}$) increase in the order $CH_3\cdots IBH_2 < CH_3\cdots IH \approx CH_3\cdots ICH_3 \approx CH_3\cdots IC_2H_3 < CH_3\cdots ICCH < CH_3\cdots ICN < CH_3\cdots INC$ at both the B3LYP/6-311++G** and MP2/aug-*cc*-pVTZ levels. This indirectly suggests that the two theoretical levels selected here are feasible and reliable.

2.2 Interaction energies and stability

Examining the interaction energy is a powerful approach for estimating the strength of a weak interaction. The single-electron iodine-bond interaction energies of the $CH_3\cdots I—Y$ (Y = BH_2, H, CH_3, C_2H_3, CCH, CN, and NC) complexes at the B3LYP/6-311++G** and MP2/aug-*cc*-pVTZ levels are listed in Table 2. The BSSE correction is taken into consideration because this is a necessary step for accurately describing the energies of weak interaction systems. As shown in Table 2, the BSSEs obtained using the MP2 method, ranging from 0.91 to 15.36 kJ mol^{-1}, are obviously larger than those of the B3LYP method. Both ΔE_{CP} (B3LYP) and ΔE_{CP} (MP2) are smaller than those of the energies without BSSE correction (ΔE); in particular, the differences obtained with the MP2 method are relatively large and non-negligible. Obviously, it is necessary to perform a CP

Table 1 Stretching vibrational frequency (cm^{-1}), frequency shift (cm^{-1}, in italics in brackets), and IR intensity (km mol^{-1}, in regular type in brackets) of the C—H, I—Y (Y = BH_2, H, CH_3, C_2H_3, CCH, CN, and NC) bonds

Compound	Parameter	B3LYP/6-311++G**[a)]	MP2/aug-*cc*-pVTZ[a)]
CH_3	υ_{C-H}	3281.29 (4.8)	3367.2(1.8)
IBH_2	υ_{I-B}	579.95 (45.6)	624.8(46.1)[b)]
IH	υ_{I-H}	2305.5 (4.3)	2641.9(1.1)
ICH_3	υ_{I-C}	508.4 (4.9)[c)]	660.3(0.3)
IC_2H_3	υ_{I-C}	514.1 (17.3)	632.7(4.6)
ICCH	υ_{I-C}	490.1 (0.5)	566.7(0.8)
ICN	υ_{I-C}	472.1 (0.4)	550.2(0.4)
INC	υ_{I-N}	448.9 (2.2)	549.6(11.4)
$CH_3\cdots IBH_2$	$\upsilon_{C\cdots I}$, υ_{I-B}	12.51(0.03), 579.97(41.1, *0.02*)	31.6(0.02), 624.7(47.3, *–0.1*)[b)]
$CH_3\cdots IH$	$\upsilon_{C\cdots I}$, υ_{I-H}	46.9(0.4), 2288.2(30.9, *–17. 3*)	72.4(0.16), 2615.4(7.7, *–26.5*)
$CH_3\cdots ICH_3$	$\upsilon_{C\cdots I}$, υ_{I-C}	46.7(0.6), 505.3(0.78, *–3.1*)[c)]	71.2(0.31), 657.6(0.7, *–2.7*)
$CH_3\cdots IC_2H_3$	$\upsilon_{C\cdots I}$, υ_{I-C}	45.4(0.5), 512.6(10.9, *–1.5*)	67.8(0.2), 641.4(4.3, *8.7*)
$CH_3\cdots ICCH$	$\upsilon_{C\cdots I}$, υ_{I-C}	70.2 (1.7), 477.3(9.7, *–12.8*)	82.0(0.6), 569.5(1.5, *2.8*)
$CH_3\cdots ICN$	$\upsilon_{C\cdots I}$, υ_{I-C}	91.8(4.0), 447.3(17.2, *–24.8*)	87.8(1.5), 558.5(21.9, *8.3*)
$CH_3\cdots INC$	$\upsilon_{C\cdots I}$, υ_{I-N}	124.3 (10.7), 383.5(41.1, *–65.4*)	99.8(6.4), 452.4(41.1, *–97.2*)

a) The relativistic ECP basis set of lanl2dz was used for iodine atom; b) data obtained on the basis set of 6-311++G** which was used for the boron, carbon and hydrogen atoms; c) data obtained on the basis set of 6-311++G(2d, 2p) which was used for the carbon and hydrogen atoms.

Table 2 BSSE-corrected interaction energies (kJ mol^{-1}) for the seven complexes at different computational levels

Compound	B3LYP/6-311++G**			MP2/aug-*cc*-pVTZ		
	ΔE	BSSE	ΔE_{CP}	ΔE	BSSE	ΔE_{CP}
$CH_3\cdots IBH_2$	−0.10	0.17	0.07	−1.48	0.91	−0.57
$CH_3\cdots IH$	−1.58	0.70	−0.88	−7.32	5.96	−1.36
$CH_3\cdots ICH_3$	−8.00	1.23	−6.77	−7.37	3.57	−3.80
$CH_3\cdots IC_2H_3$	−2.03	0.88	−1.15	−6.65	4.48	−2.17
$CH_3\cdots ICCH$	−5.48	1.60	−3.88	−9.31	4.82	−4.49
$CH_3\cdots ICN$	−8.89	1.48	−7.41	12.19	5.86	−6.33
$CH_3\cdots INC$	−19.54	2.07	−17.47	−24.00	15.36	−8.64

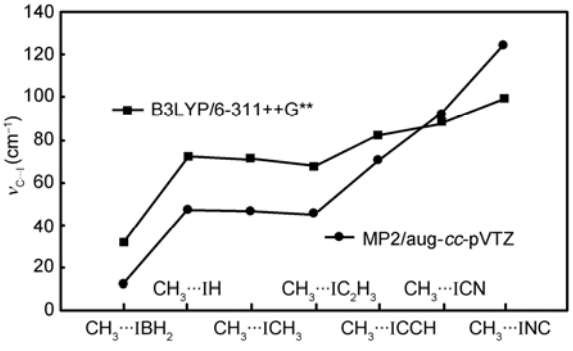

Figure 4 Comparison of $\upsilon_{C\cdots I}$ calculated at the B3LYP/6-311++G** and MP2/aug-*cc*-pVTZ levels.

correction when the MP2 method is used.

Furthermore, as shown in Figure 5, except for the interaction energy of the complex $CH_3\cdots ICH_3$, the interaction energies of the other complexes obtained using the MP2/aug-*cc*-pVTZ method are linearly correlated to those obtained by the B3LYP/6-311++G** method, and the relevant equation is $y = 1.0374x - 3.6539$ ($R^2 = 0.9638$). In

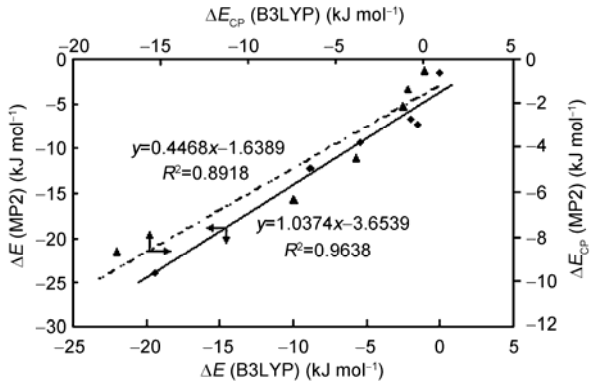

Figure 5 Linear relationships between ΔE (B3LYP) and ΔE (MP2), ΔE_{CP} (B3LYP) and ΔE_{CP} (MP2).

fact, the relationship between ΔE_{CP} (B3LYP) and ΔE_{CP} (MP2) is also linear ($y = 0.4468x - 1.6389$, $R^2 = 0.8918$). These results may also suggest that the selected theoretical methods used here are reliable. Additionally, by comparing the BSSE-corrected interaction energies (ΔE_{CP}) of the SEXB complexes, except for that of $CH_3\cdots ICH_3$, it can easily be found that the relative stabilities of the six complexes increase in the order $CH_3\cdots IBH_2 < CH_3\cdots IH \approx CH_3\cdots IC_2H_3 < CH_3\cdots ICCH < CH_3\cdots ICN < CH_3\cdots INC$, which is consistent with the increasing order of the C···I stretching frequencies ($\upsilon_{C\cdots I}$).

Compared with single-electron Br-bond systems, the single-electron iodine-bond has a larger interaction energy. For example, the single-electron Br-bond interaction energies (ΔE_{CP}, MP2) in the $CH_3\cdots BrH$, $CH_3\cdots BrC_2H_3$, $CH_3\cdots BrCCH$, $CH_3\cdots BrCN$, and $CH_3\cdots BrNC$ complexes are −1.26, −0.38, −2.95, −4.35, and −7.33 kJ mol^{-1}, respectively [11]; the single-electron iodine-bond interaction energies (ΔE_{CP}, MP2) in the $CH_3\cdots IH$, $CH_3\cdots IC_2H_3$, $CH_3\cdots ICCH$,

$CH_3\cdots ICN$, and $CH_3\cdots INC$ complexes are −1.36, −2.17, −4.49, −6.33, and −8.64 kJ mol^{-1}, respectively. This supports our viewpoint, described in the introduction, that iodine would be more suitable than Br as an electron acceptor in SEXB systems. In other words, this implies that a single-electron iodine-bond complex is more stable than a single-electron Br-bond complex.

For the sake of accuracy of the interaction energies, the ECP basis set of SDD was also used on the iodine atoms. For example, the interaction energies without BSSE correction (ΔE) of the $CH_3\cdots IH$, $CH_3\cdots ICH_3$, $CH_3\cdots ICN$, and $CH_3\cdots INC$ complexes obtained using MP2/aug-*cc*-pVTZ/SDD are −6.58, −7.62, −12.81, and −25.45 kJ mol^{-1}, respectively; these are similar to those for the MP2/aug-*cc*-pVTZ/Lanl2dz computational level. Thus the ECP basis set of Lanl2dz is reliable and adequate for iodine atoms in the present SEXB systems.

2.3 NBO analysis and NMR properties

For a better understanding of the mechanism of formation of SEXB complexes, NBO analysis was performed for the monomers and complexes at the B3LYP/6-311++G** level, and the corresponding results are listed in Table 3. The interaction strength between the monomers could be clarified according to the second-order stabilization energy $E_{ij}^{(2)}$ obtained from the NBO analysis as follows

$$E_{ij}^{(2)} = -\eta_\sigma \frac{\langle \sigma^* | F | \sigma \rangle}{\varepsilon_{\sigma^*} - \varepsilon_\sigma} = \eta_\sigma \frac{F_{ij}^2}{\Delta E}, \quad (1)$$

where F_{ij} is the Fock matrix element between the i and j NBO orbitals, ε_σ and ε_{σ^*} are the energies of σ and σ^*, and η_σ is the population of the donor σ orbital. As NBO theory indicates, electron transfer among orbitals accompanies the formation of a noncovalent bond and has a major role in the formation, so the $E_{ij}^{(2)}$ can be taken as an index to judge the strength of a noncovalent interaction. Generally, the larger the stabilization energy $E_{ij}^{(2)}$, the stronger the interaction between the donor and acceptor orbitals. As shown in Table 3, there are two kinds of charge transfer in the seven complexes. One is from I—Y to the CH_3 radical, including LP(I) → LP*(C) and (I—Y) → LP*(C); the other is from the CH_3 radical to I—Y, including LP(C) → σ^*(I—Y) and (C—H)→ σ^*(I—Y). The $E_{ij}^{(2)}$ of the latter kind is obviously larger than that of the former, thus the total charge transfer direction is from the CH_3 radical to the I—Y fragments. Among these interactions between donor and acceptor orbitals, LP(C) → σ^*(I—Y) is the most important, and it determines the nature of the SEXBs. The total amount of NBO charge transfer (Δ_{NC}) from the CH_3 radical to I—Y increases in the order $CH_3\cdots IBH_2 < CH_3\cdots IH \approx CH_3\cdots ICH_3 \approx CH_3\cdots IC_2H_3 < CH_3\cdots ICCH < CH_3\cdots ICN < CH_3\cdots INC$. It is also interesting to find that the p character of the hybridization of the C atom in C···I SEXBs changes in the following order: $CH_3\cdots IBH_2 \approx CH_3\cdots IH \approx CH_3\cdots ICH_3 \approx CH_3\cdots IC_2H_3 < CH_3\cdots ICCH < CH_3\cdots ICN < CH_3\cdots INC$, which approximates to the increasing order of the total amount of NBO charge transfer (Δ_{NC} (CH_3 → I—Y)).When two systems A and B are bonded together, a single system will be formed with a constant μ value (chemical potential). In this case, there is an electron transfer from the less electronegative system to the other and the fractional number of electrons transferred (ΔN) is given as follows [22]: $\Delta N = (\chi_A - \chi_B)/2(\eta_A + \eta_B)$, where χ ($\chi = -\mu$) is the absolute electronegativity and η is the chemical hardness; μ and η are important quantities and they are used to characterize any chemical system. They are defined as $\mu = (I + A)/2$ and $\eta = (I - A)/2$, where I and A are the ionization energy and electron affinity of the system. In addition, according to Koopmans's law [23], μ and η can also be defined as follows: $\mu = (E_{LUMO} + E_{HOMO})/2$; $\eta = (E_{LUMO} - E_{HOMO})/2$, where E_{LUMO} and E_{HOMO} are the energy levels of the LUMO and HOMO, respectively. Generally, a large value of ΔN represents a strong and favorable interaction between A and B. The ΔN values obtained using Koopmans's law, listed in Table 3 for the complexes, are all smaller than 0.4, which indicates that electron transfers from CH_3 to I—Y are all weak. This is consistent with the fact that SEXB binding energies are small. On the other hand, the small ΔN values predict that the charge-transfer energy is only a small contribution to the total

Table 3 NBO analysis for the complexes at the B3LYP/6-311++G** computational level

	$CH_3\cdots IBH_2$	$CH_3\cdots IH$	$CH_3\cdots ICH_3$	$CH_3\cdots IC_2H_3$	$CH_3\cdots IC_2H$	$CH_3\cdots ICN$	$CH_3\cdots INC$
$E_{ij}^{(2)}$LP(I)→LP*(C)[a] (kJ/mol)	0.13	1.51	1.72	1.72	3.61	6.17	16.04
$E_{ij}^{(2)}$ σ(I—Y)→LP*(C) (kJ/mol)	0.00	0.59	0.71	0.46	0.46	0.67	1.09
$E_{ij}^{(2)}$LP(C)→σ^*(I—Y) (kJ/mol)	0.42	5.29	4.96	4.28	8.23	16.21	50.48
$E_{ij}^{(2)}\sigma$(C—H)→σ^*(I—Y) (kJ/mol)	0.00	0.00	0.76	0.76	1.52	2.98	10.21
$C(sp^n)_{C-H}$	$sp^{2.00}$	$sp^{2.00}$	$sp^{2.00}$	$sp^{2.00}$	$sp^{2.02}$	$sp^{2.03}$	$sp^{2.10}$
$\Delta_{NC}(CH_3\rightarrow I-Y)$ (me)	1	6	7	8	17	35	86
ΔN	0.1387	0.0793	0.0480	0.0642	0.0811	0.2977	0.3809
Bond order$_{C\cdots I}$	0.0000	0.0048	0.0032	0.0013	0.0058	0.0058	0.1750
Dipole moments (Deby)	0.5551	0.6439	1.4185	0.9848	0.9681	4.9359	6.0737

a) LP represents lone pair electron orbital, LP* represents non-bond electron orbital.

binding energy. Therefore, the polarization, including dispersion and induction contributions, is perhaps very important to the total binding energy. In fact, the charge transfers from the donor to acceptor orbital and the coupling thereof are often small, but they are significant for the analysis of the nature of intermolecular weak interactions. In addition, it is noted that the ΔN value of $CH_3\cdots IBH_2$ is larger than those of $CH_3\cdots IH$, $CH_3\cdots ICH_3$, $CH_3\cdots IC_2H_3$, and $CH_3\cdots ICCH$, which is a discrepancy with respect to the Δ_{NC} values, the C···I stretching frequencies ($\upsilon_{C\cdots I}$), and the relative interaction energies; that is, the value of ΔN is not always suitable for predicting the relative strengths of the seven SEXB interaction systems in the present study. However, for the $CH_3\cdots ICH_3$, $CH_3\cdots IC_2H_3$, $CH_3\cdots ICCH$, $CH_3\cdots ICN$, and $CH_3\cdots INC$ systems, the sequence of their ΔN values is consistent with that of their Δ_{NC} values, which suggests that the ΔN values can be used to describe the relative interaction strengths for these five complexes.

Figure 6(a) and (b) show that the dipole moments of the complexes correlate with the interaction energies ΔE and ΔE_{CP} at the B3LYP/6-311++G** level, respectively. The shapes of the two curves are very similar, which suggests that the greater the dipole moment of the complex, the more nonsymmetrical the charge distribution, the more negative the interaction energy, the stronger the interaction, and the more stable the SEXB interaction system.

To further investigate the essence of SEXB interactions, the sources and the energies of the frontal molecular orbitals of $CH_3\cdots I—Y$ ($CH_3\cdots ICH_3$ and $CH_3\cdots ICN$) are shown in Figure 7. For the $CH_3\cdots ICH_3$ complex, the HOMO and HOMO-1 come from HOMO and HOMO-1 of the CH_3I moiety, respectively, but the HOMO-2 comes from the HOMO of the CH_3 radical. Thus the CH_3 radical becomes more stable after SEXB formation. For the $CH_3\cdots ICN$ complex, the sources of its LUMO, HOMO, and HOMO-1 are similar to those of the $CH_3\cdots ICH_3$ complex, but the sources of HOMO-2 of the two complexes are different. The source of the HOMO-2 of the $CH_3\cdots ICN$ complex comes from two moieties, namely the HOMO of the CH_3 radical and the HOMO-2 of the ICN moiety. Thus, the $CH_3\cdots ICN$ complex will be more stable than the $CH_3\cdots ICH_3$ complex. For the sake of brevity, the sources of the frontal molecular orbitals of the other complexes are not given here.

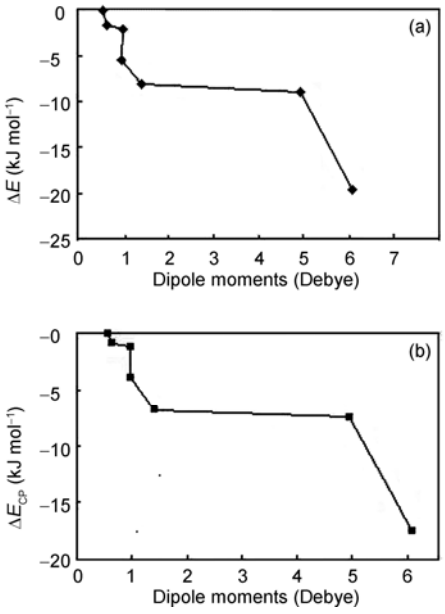

Figure 6 Relationship between ΔE and dipole moments (a), and ΔE_{CP} and dipole moments (b).

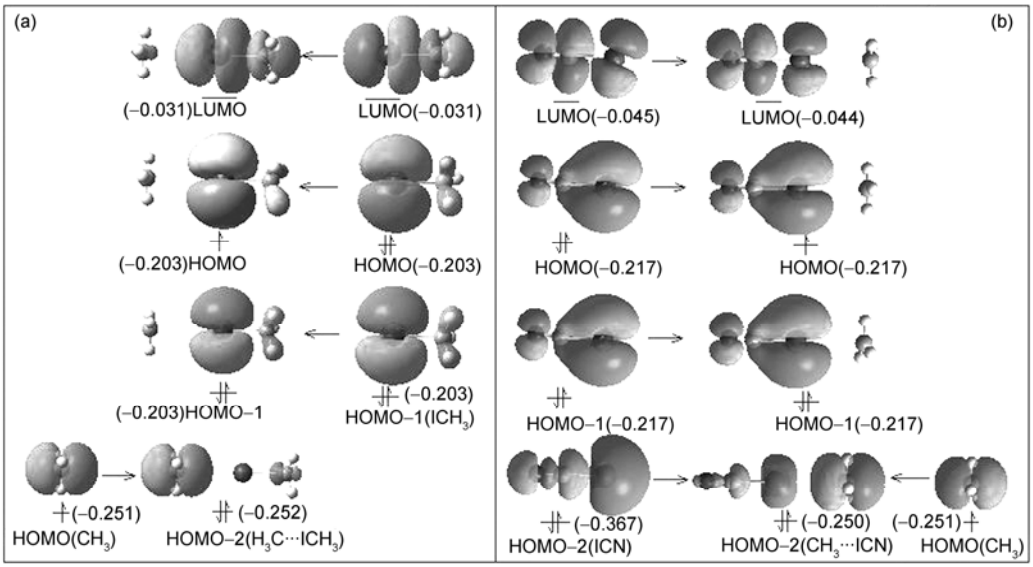

Figure 7 Sources of frontal molecular orbitals in complexes $CH_3\cdots ICH_3$ (a) and $CH_3\cdots ICN$ (b).

2.4 AIM and MEP analysis

The topological properties of the scalar field electron density ($\rho(r)$) can be described by the numbers and the categories of the critical points. A critical point is the spatial position where the first derivative of the $\rho(r)$ is zero, as follows

$$\nabla\rho(r) = i\frac{\partial}{\partial x}\rho(r) + j\frac{\partial}{\partial y}\rho(r) + k\frac{\partial}{\partial z}\rho(r) = 0 . \quad (2)$$

The type of the critical point can be defined according to the critical point curvature obtained by calculating the second derivative of the $\rho(r)$. The Hessian matrix of the electron density is composed of nine secondary derivatives of $\rho(r)$ in three dimensions. The three eigenvalues (λ_1, λ_2, and λ_3) can be acquired by performing a diagonalized operator on the Hessian matrix. The sum of the three eigenvalues is equal to the Laplacian of the electron density ($\nabla^2\rho(r) = \lambda_1 + \lambda_2 + \lambda_3$). Among the three eigenvalues, if two of them are negative and the other is positive, the corresponding critical point is designated as the bond critical point (BCP) and marked as (3, −1), indicating the linkage between the two atoms; if two of them are positive and the other is negative, the corresponding critical point is designated as the ring critical point, and marked as (3, +1), indicating the existence of a ring structure. The nuclear position is marked as (3, −3). According to Bader's AIM theory [24], the electron density topological properties of a molecule depend on the electron density gradient vector field and $\nabla^2\rho(r)$. In general, the electron density of a BCP ($\rho(r_c)$) is related to the strength of the bond: the larger the $\rho(r_c)$ is, the stronger the bond; the smaller the $\rho(r_c)$ is, the weaker the bond. The $\nabla^2\rho(r)$ of the BCP reflects the characteristics of the bond. If $\nabla^2\rho(r_c)<0$, the BCP charges will be concentrated, and the more negative $\nabla^2\rho(r_c)$ is, the more covalent the property is; if $\nabla^2\rho(r_c)>0$, the BCP charges will be dispersed, and the more positive $\nabla^2\rho(r_c)$ is, the more ionic the property is.

The electron density topological properties of the SEXB critical points in the seven complexes are listed in Table 4. The three eigenvalues of the electron density Hessian matrix of C···I are "one positive and two negative". Therefore, the critical points between the atom pairs of C···I belong to the type BCP. The $\rho(r)$ values of C···I in the seven complexes are smaller than 0.021 a.u. This indicates that the SEXB interactions in the seven complexes are weak, which is in good agreement with the calculation results for the interaction energies. Furthermore, it is noted that the $\rho(r)$ of the C···I in the seven complexes is related to the amounts of Δ_{NC} (CH3 → I—Y), that is, the larger the Δ_{NC}, the larger the ρ(r) of the C···I atom pair. The relationship between Δ_{NC} and $\rho(r)$ is linear ($y = 0.0002x + 0.0034$, with $R^2 = 0.9708$) (Figure 8(a)). In addition, the $\nabla^2\rho(r)$ of the corresponding critical points are all small negative values (more than –0.012 a.u.), which shows that this kind of weak interaction has a few covalent property. The ellipticity, ε, is defined as λ_1/λ_2-1, in which λ_1 and λ_2 are the two eigenvalues of the Hessian matrix of electron density. The ellipticity provides a measure for the σ or π character of a bond. In general, the smaller ε is, the stronger the σ character is, and conversely for the π character. Figure 8 (b) shows the relevance between ε and $\nabla^2\rho(r_c)$, which is $y = 0.0018\ln(x) - 0.0028$ ($R^2 = 0.7589$) suggesting that the covalent property of the C···I atom pair is mainly σ in character.

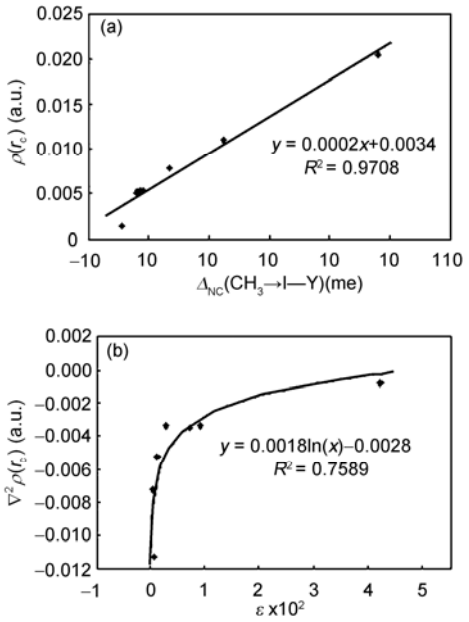

Figure 8 Linear relationship between $\rho(r_c)$ (a.u.) and Δ_{NC} (CH_3→I—Y) (me) (a), $\nabla^2\rho(r_c)$ (a.u.) and ε(seven)(b).

Table 4 Electron density topological properties of bond critical points for the seven complexes

Compound	Atom pair	$\rho(r_c)$ (a.u.)	λ_1	λ_2	λ_3	$\nabla^2\rho(r_c)$ (a.u.)	ε
CH_3···IBH_2	I···C	0.00142	–0.00057	–0.00055	0.00431	–0.00080	0.04196
CH_3···IH	I···C	0.00510	–0.00232	–0.00231	0.01792	–0.00332	0.00274
CH_3···ICH_3	I···C	0.00538	–0.00245	–0.00243	0.01872	–0.00346	0.00704
CH_3···IC_2H_3	I···C	0.00533	–0.00247	–0.00245	0.01832	–0.00335	0.00902
CH_3···ICCH	I···C	0.00786	–0.00399	–0.00398	0.02902	–0.00526	0.00109
CH_3···ICN	I···C	0.01101	–0.00609	–0.00609	0.04110	–0.00723	0.00041
CH_3···INC	I···C	0.02053	–0.01295	–0.01295	0.07113	–0.01130	0.00048

3 Conclusions

In the present study, the iodine-involved weak interactions in systems $CH_3\cdots I—Y$ (Y = BH_2, H, CH_3, C_2H_3, CCH, CN, and NC) were investigated at the MP2/aug-*cc*-pVTZ and B3LYP/6-311++G** computational levels (the relativistic ECP basis set of Lanl2dz was used on the iodine atom) for the first time. In the seven complexes, SEXB structures were formed via the iodine atom of I—Y (Y = BH_2, H, CH_3, C_2H_3, CCH, CN, and NC) as the electron acceptor (but the SEXB donor) and the CH_3 radical as the electron donor. By comparing the BSSE-corrected interaction energies (ΔE_{CP}) of the SEXB complexes, it can be easily found that the relative stabilities of the seven complexes increased in the order $CH_3\cdots IBH_2 < CH_3\cdots IH \approx CH_3\cdots IC_2H_3 < CH_3\cdots ICH_3 < CH_3\cdots ICCH < CH_3\cdots ICN < CH_3\cdots INC$, which is consistent with the increasing sequence of the C···I stretching frequencies ($\upsilon_{C\cdots I}$). In the NBO analysis, the total amount of NBO charge transfer (Δ_{NC}) from the CH_3 radical to I—Y increases in the order $CH_3\cdots IBH_2 < CH_3\cdots IH \approx CH_3\cdots ICH_3 \approx CH_3\cdots IC_2H_3 < CH_3\cdots ICCH < CH_3\cdots ICN < CH_3\cdots INC$. AIM analysis showed that the $\rho(r)$ values of C···I in the seven complexes are smaller than 0.021 a.u. This indicates that the SEXB interactions are weak, which in good agreement with the calculated results for interaction energies.

This work was supported by the Key Project of the Chinese Ministry of Education (211189), the National Natural Science Foundation of China (51063006), and the "QingLan" Talent Engineering Funds of Tianshui Normal University.

1 Zhao Y, Truhlar D G. Assessment of model chemistries for noncovalent interactions. J Chem Theory Comput, 2006, 2: 1009–1018
2 Yang Y, Zhang W J. Theoretical study of N—H···H—B blue-shifted dihydrogen bond. J Mol Struct, 2007, 814: 113–117
3 Dunbar R C. Complexation of Na^+ and K^+ to aromatic amino acids: A density functional computational study of cation-π interactions. J Phys Chem A, 2000, 104: 8067–8074
4 Kevin E R, Pavel H. Investigations into the nature of halogen bonding including symmetry adapted perturbation theory analyses. J Chem Theory Comput, 2008, 4: 232–242
5 Feng Y, Liu L, Wang J T, et al. Blue-shifted lithium bonds. Chem Commun, 2004, 1: 88–89
6 Igarashia M, Ishibashia T, Tachikawa H. A direct *ab initio* molecular dynamics study of the finite temperature effects on the hyperfine coupling constant of methyl radical-water complexes. J Mol Struct, 2002, 594: 61–69
7 Tang K, Shi F Q. Comparative analysis of blue-shifted hydrogen bond versus conventional hydrogen bond in methyl radical complexes. Int J Quantum Chem, 2007, 107: 665–669
8 Li Y, Wu D, Li Z R, et al. Do single-electron lithium bond exist? Prediction and characterization of the $H_3C\cdots Li—Y$(Y = H, F, OH, CN, NC, and CCH) complexes. Phys Chem Chem Phys, 2006, 125: 84317–84323
9 Li Z F, Zhu Y C, Li H X. Prediction and characterization of the single-electron sodium bond complexes Y—C···Na—H (Y = N_3, H_3CH_2, $(H_3C)_2H$ and $(H_3C)_3$). Phys Chem Chem Phys, 2009, 11: 11113–11120
10 Li Q Z, An X L, Gong B A, et al. Non-additivity of methyl group in the single-electron halogen bond of CH_3—BrH complex. J Mol Struct, 2008, 866: 11–14
11 Li Z F, Shi X N, Li H Y, et al. Theoretical study of the interaction mechanism of single-electron halogen bond complexes $H_3C\cdots Br—Y$ (Y = H, CN, NC, CCH, C_2H_3). Sci China Chem, 2010, 40: 52–62
12 Wang Y H, Zou J W, Lu Y X, et al. Single-electron halogen bond: *Ab initio* study. Int J Quantum Chem, 2007, 107: 501–506
13 Su M D, Chu S Y. Density functional study of some germylene insertion reactions. J Am Chem Soc, 1999, 121: 4229–4237
14 Pluth M D, Bergman R G, Raymond K N. Encapsulation of protonated diamines in a water-soluble, chiral, supramolecular assembly allows for measurement of hydrogen-bond breaking followed by nitrogen inversion/rotation. J Am Chem Soc, 2008, 130: 6362–6366
15 Nagy P I, Erhardt P W. *Ab initio* study of hydrogen-bond formation between aliphatic and phenolic hydroxy groups and selected amino acid side chains. J Phys Chem A, 2008, 112: 4342–4354
16 Boys S F, Bernardi F. The calculation of small molecular interactions by differences of separate total energies. Some procedures with reduced errors. Mol Phys, 1970, 19: 553–556
17 Bader R F W. Atoms in Molecules: A Quantum Theory. New York: Clarendon Press, 1990
18 Biegler-Koning F J, Derdau R, Bayles D. AIM 2000, Version 1[CP]. Hamilton: McMaster University, 2000
19 Glendening E D, Badenhoop J K, Reed A E, et al. Natural Bond Orbital Program. Version 5.0. Madison, WI: Theoretical Chemistry Institute, University of Wisconsin, 2001
20 Frisch M J, Trucks G W, Schlegel H B, et al. Gaussian 03 E. 01, Pittsburgh PA: Gaussian Inc, 2004
21 Bondi A. Van der Waals volumes and radii. J Phys Chem, 1964, 68: 441–451
22 Parr R G, Pearson R G. Absolute hardness: Companion parameter to absolute electronegativity. J Am Chem Soc, 1983, 105: 7512–7516
23 Pearson R G. Chemical Hardness-Applications from Molecules to Solids. Weinheim: VCH-Wiley, 1997
24 Bader R F W. A quantum theory of molecular structure and its applications. Chem Rev, 1991, 91: 893–928